結　語

LVD, ADV, ETV のいずれにも耐性を示す多剤耐性変異出現例による BTH を発症した悪性リンパ腫合併B型慢性肝炎に対して, TDF が著効した一例を経験した. 今後, わが国でも核酸アナログ製剤投与の長期化に伴い, 多剤耐性変異を有する症例の出現が予測されることから, HBV に対する TDF 保険承認が待たれる.

謝辞：臨床データをご提供いただいた, 愛知県立がんセンター血液・細胞療法部　田地浩史先生に深謝いたします.

文　献

1) Lai CL, Chien RN, Leung NW, et al. A one-year trial of lamivudine for chronic hepatitis B. Asia Hepatitis Lamivudine Study Group. N Engl J Med 1998; 339: 61—68
2) Dienstag JL, Goldin RD, Heathcote EJ, et al. Histological outcome during long-term lamivudine therapy. Gastroenterology 2003; 124: 105—117
3) Hadziyannis SJ, Tassopoulos NC, Heathcote EJ, et al. Adefovir dipivoxil for the treatment of hepatitis B e antigen-negative chronic hepatitis B. N Engl J Med 2003; 348: 800—807
4) Marcellin P, Chang TT, Lim SG, et al. Adefovir dipivoxil for the treatment of hepatitis B e antigen-positive chronic hepatitis B. N Engl J Med 2003; 348: 808—816
5) Chang TT, Gish RG, de Man R, et al. A comparison of entecavir and lamivudine for HBeAg-positive chronic hepatitis B. N Engl J Med 2006; 354: 1001—1010
6) Lai CL, Shouval D, Lok AS, et al. Entecavir versus lamivudine for patients with HBeAg-negative chronic hepatitis B. N Engl J Med 2006; 354: 1011—1020
7) Zoulim F, Locarnini S. Hepatitis B virus resistance to nucleos (t) ide analogues. Gastroenterology 2009; 137: 1593—1608 e1-2
8) Yeo W, Johnson PJ. Diagnosis, prevention and management of hepatitis B virus reactivation during anticancer therapy. Hepatology 2006; 43: 209—220
9) Ying C, De Clercq E, Nicholson W, et al. Inhibition of the replication of the DNA polymerase M550V mutation variant of human hepatitis B virus by adefovir, tenofovir, L-FMAU, DAPD, penciclovir and lobucavir. J Viral Hepat 2000; 7: 161—165
10) Marcellin P, Heathcote EJ, Buti M, et al. Tenofovir disoproxil fumarate versus adefovir dipivoxil for chronic hepatitis B. N Engl J Med 2008; 359: 2442—2455
11) Heathcote EJ, Marcellin P, Buti M, et al. Three-year efficacy and safety of tenofovir disoproxil fumarate treatment for chronic hepatitis B. Gastroenterology 2011; 140: 132—143
12) Choe WH, Kwon SY, Kim BK, et al. Tenofovir plus lamivudine as rescue therapy for adefovir-resistant chronic hepatitis B in hepatitis B e antigen-positive patients with liver cirrhosis. Liver Int 2008; 28: 814—820
13) van Bommel F, de Man RA, Wedemeyer H, et al. Long-term efficacy of tenofovir monotherapy for hepatitis B virus-monoinfected patients after failure of nucleoside/nucleotide analogues. Hepatology 2010; 51: 73—80
14) Patterson SJ, George J, Strasser SI, et al. Tenofovir disoproxil fumarate rescue therapy following failure of both lamivudine and adefovir dipivoxil in chronic hepatitis B. Gut 2011; 60: 247—254

A case report of successful therapy with tenofovir for a multi-drug resistant chronic hepatitis B patient complicated with malignant lymphoma

Tsunamasa Watanabe[1], Fuminaka Sugauchi[2], Shigeru Kusumoto[3], Noboru Shinkai[4],
Etsuko Iio[1][4], Kentarou Matsuura[4], Atsunori Kusakabe[4], Tomokatsu Miyaki[4],
Syunsuke Nojiri[4], Yasuhito Tanaka[1]*

A 33-year-old man who diagnosed with malignant lymphoma was treated with lamivudine (LVD) for chronic hepatitis B in 2001. Because he experienced the first breakthrough hepatitis in 2005, adefovir (ADV) was added to the LVD regimen for dual therapy. In September 2007, LVD plus ADV combination therapy was replaced by entecavir (ETV) monotherapy. Eight months later, in May 2008, hepatitis B virus (HBV) DNA level elevated, followed by the second breakthrough hepatitis. After then, switching from ETV to LVD plus ADV could not suppress HBV-DNA level and ALT flare because sequencing analysis showed the evidence of multiple drug resistance with L80I, L180M, A181T, T184I and M204I/V mutations. In this case, after getting the approval of the ethical committee, we applied him the combination therapy with LVD and tenofovir (TDF), that decreased the serum HBV DNA and ALT concentration within a few months and obtained the complete remission of malignant lymphoma by allogenic bone marrow transplantation.

Key words: tenofovir multi-drug resistant mutation breakthrough hepatitis
chronic hepatitis B allogeneic bone marrow transplantation

Kanzo 2012; 53: 35—41

---

1) Department of Virology & Liver Unit, Nagoya City University Graduate School of Medical Sciences
2) Department of Gastroenterology, Nagoya City Koseiin Medcial Welfare Center
3) Department of Medical Oncology and Immunology, Nagoya City University Graduate School of Medical Sciences
4) Department of Gastroenterology and Metabolism, Nagoya City University Graduate School of Medical Sciences
*Corresponding author: ytanaka@med.nagoya-cu.ac.jp

HEPATOLOGY
Official Journal of the American Association for the Study of Liver Diseases

Severe Necroinflammatory Reaction Caused by Natural Killer Cell-Mediated Fas/Fas Ligand Interaction and Dendritic Cells in Human Hepatocyte Chimeric Mouse

Akihito Okazaki,[1,2] Nobuhiko Hiraga,[1,2] Michio Imamura,[1,2] C. Nelson Hayes,[1,2,3] Masataka Tsuge,[1,2] Shoichi Takahashi,[1,2] Hiroshi Aikata,[1,2] Hiromi Abe,[1,2,3] Daiki Miki,[1,2,3] Hidenori Ochi,[1,2,3] Chise Tateno,[2,4] Katsutoshi Yoshizato,[2,4] Hideki Ohdan,[2,5] and Kazuaki Chayama[1,2,3]

The necroinflammatory reaction plays a central role in hepatitis B virus (HBV) elimination. Cluster of differentiation (CD)8-positive cytotoxic T lymphocytes (CTLs) are thought to be a main player in the elimination of infected cells, and a recent report suggests that natural killer (NK) cells also play an important role. Here, we demonstrate the elimination of HBV-infected hepatocytes by NK cells and dendritic cells (DCs) using urokinase-type plasminogen activator/severe combined immunodeficiency mice, in which the livers were highly repopulated with human hepatocytes. After establishing HBV infection, we injected human peripheral blood mononuclear cells (PBMCs) into the mice and analyzed liver pathology and infiltrating human immune cells with flow cytometry. Severe hepatocyte degeneration was observed only in HBV-infected mice transplanted with human PBMCs. We provide the first direct evidence that massive liver cell death can be caused by Fas/Fas ligand (FasL) interaction provided by NK cells activated by DCs. Treatment of mice with anti-Fas antibody completely prevented severe hepatocyte degeneration. Furthermore, severe hepatocyte death can be prevented by depletion of DCs, whereas depletion of CD8-positive CTLs did not disturb the development of massive liver cell apoptosis. *Conclusion:* Our findings provide the first direct evidence that DC-activated NK cells induce massive HBV-infected hepatocyte degeneration through the Fas/FasL system and may indicate new therapeutic implications for acute severe/fulminant hepatitis B. (HEPATOLOGY 2012;56:555-566)

Between 4% and 32% of fulminant hepatitis cases, characterized by acute massive hepatocyte degeneration and subsequent development of hepatic encephalopathy and liver failure, are caused by acute hepatitis B virus (HBV) infection.[1] Host[2] and viral factors[3] may influence the development of fulminant hepatitis, but these factors have not been fully elucidated.

Innate and adaptive immunity both play a role in the elimination of viral infections. In the innate immune response, cytoplasmic and membrane-bound receptors recognize viruses and induce interferon (IFN)-β production, which, in turn, up-regulates IFN-α and induces an antiviral state in surrounding cells.[4] In the adaptive immune response, viruses are recognized by dendritic cells (DCs), which activate cluster of differentiation (CD)8-positive T cells to reduce viral replication through cytolytic[5] and noncytolytic mechanisms.[6] The role of immune cells, especially HBV-specific cytotoxic T lymphocytes (CTLs), is crucial in the

---

Abbreviations: APC, allophycocyanin; asialo GM1, ganglio-N-tetraosylceramide; CD, cluster of differentiation; CHB, chronic hepatitis B; CTLs, cytotoxic T lymphocytes; DC, dendritic cell; FasL, Fas ligand; FHB, fulminant hepatitis B; HBcAg, hepatitis B core antigen; HBsAg, hepatitis B surface antigen; HBV, hepatitis B virus; HLA, human leukocyte antigen; HSA, human serum albumin; IFN, interferon; IP, intraperitoneally; ISG, interferon-stimulated gene; mAb, monoclonal antibody; mDC, myeloid DC; mRNA, messenger RNA; NK, natural killer; PBMCs, peripheral blood mononuclear cells; PCR, polymerase chain reaction; pDC, plasmacytoid DC; SCID, severe combined immunodeficiency; TUNEL, terminal deoxynucleotidyl transferase dUTP nick end labeling; uPA, urokinase-type plasminogen activator.

From the [1]Department of Medicine and Molecular Science, Division of Frontier Medical Science, Programs for Biomedical Research, Graduate School of Biomedical Sciences, Hiroshima University, Hiroshima, Japan; [2]Liver Research Project Center, Hiroshima University, Hiroshima, Japan; [3]Laboratory for Digestive Diseases, Center for Genomic Medicine, RIKEN, Hiroshima, Japan; [4]PhoenixBio Co., Ltd., Higashi-Hiroshima, Japan; and [5]Department of Surgery, Division of Frontier Medical Science, Programs for Biomedical Research, Graduate School of Biomedical Science, Hiroshima University, Hiroshima, Japan.

Received August 16, 2011; accepted February 4, 2012.

This study was supported, in part, by a Grant-in-Aid for Scientific Research from the Japanese Ministry of Labor, Health, and Welfare.

development of fulminant hepatitis.[7,8] CTLs can kill target cells using two distinct lytic pathways: the degranulation pathway, in which perforin is used to puncture the membranes of infected cells, and the Fas-based pathway, in which the interaction between Fas ligand (FasL) expressed on cytolytic lymphocytes and Fas on target cells triggers apoptosis and target cell death.[9] However, the role of innate immune cells, especially natural killer (NK) cells, in fulminant hepatitis remains obscure. NK cells have recently been reported to contribute to the pathogenesis of human hepatitis and animal models of liver injury.[10,11] Replication of HBV is host cell dependent, and the study of cellular immune response in hepatitis B has long been hampered by the lack of a small animal model that supports the replication of HBV and elimination of infected cells by immune response. Before the advent of human hepatocyte chimeric mice,[12,13] only chimpanzees had been used as a model for HBV infection and inflammation, although fulminant hepatitis B (FHB) had never been reported, and severe liver inflammation is rare in chimpanzees.[14] We previously established an HBV-infection animal model using chimeric mice, in which the livers were extensively repopulated with human hepatocytes.[15-17] In this study, we attempted to establish an animal model of HBV-infected human hepatocytes with human immunity by transplanting human peripheral mononuclear cells (PBMCs) to HBV-infected human hepatocyte chimeric mice.

Materials and Methods

Generation of Human Hepatocyte Chimeric Mice. Generation of the urokinase-type plasminogen activator (uPA)$^{+/+}$/severe combined immunodeficiency (SCID)$^{+/+}$ mice and transplantation of human hepatocytes with human leukocyte antigen (HLA)-A0201 were performed as described previously.[15,16] All mice were transplanted with frozen human hepatocytes obtained from the same donor. Infection, extraction of serum samples, and euthanasia were performed under ether anesthesia. Concentration of human albumin, which is correlated with the repopulation index,[15] was measured in mice as described previously.[16] All animal protocols described in this study were performed in accord with the *Guide for the Care and Use of Laboratory Animals* and the local committee for animal experiments, and the experimental protocol was approved by the Ethics Review Committee for Animal Experimentation of the Graduate School of Biomedical Sciences at Hiroshima University (Hiroshima, Japan).

Human Serum Samples. Human serum samples, containing high titers of genotype C HBV DNA (5.3 $\times$ 10^6 copies/mL), were obtained from patients with chronic hepatitis who provided written informed consent. Individual serum samples were divided into aliquots and stored in liquid nitrogen. Six weeks after hepatocyte transplantation, chimeric mice were injected intravenously with 50 μL of HBV-positive human serum.

Analysis of HBV. DNA was extracted using SMITEST (Genome Science Laboratories, Tokyo, Japan) and dissolved in 20 μL of H_2O. HBV DNA was measured by real-time polymerase chain reaction (PCR) using a light cycler (Roche, Mannheim, Germany). Primers used for amplification were 5′-TTTGGGCATGGACATTGAC-3′ and 5′-GGTGAACAATGTTCCGGAGAC-3′. Amplification conditions included initial denaturation at 95°C for 10 minutes, followed by 45 cycles of denaturation at 95°C for 15 seconds, annealing at 58°C for 5 seconds, and extension at 72°C for 6 seconds. The lower detection limit of this assay was 300 copies.

Preparation of Human Blood Mononuclear Cells and Transplantation of Human PBMCs Into Human Hepatocyte Chimeric Mice. PBMCs were isolated from healthy blood donors with HLA-A0201 and successfully vaccinated with recombinant yeast-derived hepatitis B surface antigen (HBsAg) vaccine (Bimmugen; Chemo-Sero Therapeutic Institute, Kumamoto, Japan) using Ficoll-Hypaque density gradient centrifugation. Neither monocytes nor macrophages were observed in the isolated PBMCs (Supporting Fig. 1). PBMCs isolated from 3 healthy, unvaccinated blood donors were also transplanted. Eight weeks after HBV inoculation, human PBMCs were transplanted into human hepatocyte chimeric mice. To deplete mouse NK cells and prevent the elimination of human PBMCs from human hepatocyte

---

Address reprint requests to: Kazuaki Chayama, M.D., Ph.D., Department of Medical and Molecular Science, Division of Frontier Medical Science, Programs for Biomedical Research, Graduate School of Biomedical Science, Hiroshima University, 1-2-3 Kasumi, Minami-ku, Hiroshima 734-8551, Japan. E-mail: chayama@hiroshima-u.ac.jp; fax: +81-82-255-6220.

DOI 10.1002/hep.25651

Potential conflict of interest: The authors have no conflicts to disclose.

Additional Supporting Information may be found in the online version of this article.

chimeric mice, 200 μL of phosphate-buffered saline, containing 120 μL of anti–ganglio-N-tetraosylceramide (asialo GM1) antibody (Wako, Osaka, Japan), were administered intraperitoneally (IP) 1 day before (day 0; Fig. 1) the initial IP transplantation (day 1) of human PBMC. Then, 10 μL/g of liposome-encapsulated clodronate (Sigma-Aldrich, St. Louis, MO) were also administered 4 days before PBMC transplantation (day -2) to deplete mouse macrophages and DC cells. The second PBMC administration (4×10^7 cells/mouse) was performed 2 days after the initial administration (day 3).

To assess the effect of the depletion of human DC, NK, or CD8-positive CTL cells from administered PBMCs on hepatitis formation, the BD IMag separation system (BD Biosciences, Franklin Lakes, NJ) was used. Alternatively, mice were treated with an IP administration of clodronate, as described above, 1 day before PBMC transplantation.

To analyze the effect of inhibition of the Fas/FasL system, IFN-γ, IFN-α, antihuman FasL monoclonal antibody (mAb) (1.5 mg/mouse; R&D Systems, Minneapolis, MN), antihuman IFN-γ mAb (1.5 mg/mouse; R&D Systems), and antihuman IFN-α mAb (1.5 mg/mouse; PBL Biomedical Laboratories, Piscataway, NJ) were injected 1 day before transplantation of human PBMCs.

Flow Cytometry. Reconstructed human PBMC proliferation in mice was determined by flow cytometry with the following mAbs used for PBMC surface staining: allophycocyanin (APC)-H7 antihuman CD3 (clone SK7); APC-conjugated anti-CD4 (clone SK); BD Horizon V450 antihuman CD8 (clone RPA-T8); APC-conjugated antihuman CD11c (clone B-ly6); HU HRZN V500 MAB-conjugated antihuman CD45 (clone H130); Alexa Fluor 488–conjugated antihuman CD56 (clone B159); PerCP-Cy5.5 antihuman CD123 (clone 7G3); fluorescein isothiocyanate–conjugated Lineage cocktail 1 (Lin-1) (anti-CD3, CD14, CD16, CD19, CD20, and CD56); APC-H7 antihuman HLA-DR (clone L243); phycoerythrin (PE)-conjugated antihuman FasL (clone NOK-1); and biotin-conjugated antimouse H-2D^b (clone KH95). The biotinylated mAbs were visualized using PE-Cy7-streptavidin. Each of the above mAbs were purchased from BD Biosciences. PE-conjugated HBV core-derived immunodominant CTL epitope (HBcAg93)[18] (Medical & Biological Laboratories Co., Ltd., Nagoya, Japan). Dead cells identified by light scatter and propidium iodide staining were excluded from the analysis. Flow cytometry was performed using a FACSAria II flow cytometer (BD Biosciences), and results were analyzed with FlowJo software (Tree Star, Inc., Ashland, OR).

DCs can be classified into two main subsets: plasmacytoid DCs (pDCs) and myeloid DCs (mDCs).[19,20] pDCs were defined as CD45$^+$Lin-1$^-$HLA-DR$^+$CD123$^+$ cells, whereas mDCs were defined as CD45$^+$ Lin-1$^-$HLA-DR$^+$CD11c$^+$ cells.

Histochemical Analysis of Mouse Liver and Terminal Deoxynucleotidyl Transferase dUTP Nick End Labeling Assay. Histochemical analysis and immunohistochemical staining using an antibody against human serum albumin (HSA; Bethyl Laboratories, Inc., Montgomery, TX), an antibody against hepatitis B core antigen (HBcAg) (Dako Diagnostika, Hamburg, Germany) and antibody against Fas (BD Biosciences, Tokyo, Japan) were performed as described previously.[16] Immunoreactive materials were visualized using a streptavidin-biotin staining kit (Histofine SAB-PO kit; Nichirei, Tokyo, Japan) and diainobenzidine. For the terminal deoxynucleotidyl transferase dUTP nick end labeling (TUNEL) assay in sliced tissues, we used an *in situ* cell death detection kit (POD; Roche Diagnostics Japan, Tokyo, Japan).

Dissection of Mouse Livers and Isolation of RNA and Measurement of Messenger RNAs of Fas by Reverse-Transcription PCR. Mice were sacrificed by anesthesia with diethyl ether, and livers were excised, dissected into small sections, and then snap-frozen in liquid nitrogen. Total RNA was extracted from cell lines using the RNeasy Mini Kit (Qiagen, Valencia, CA). One microgram of each RNA sample was reverse transcribed with ReverseTra Ace (Toyobo Co., Tokyo, Japan) and Random Primer (Takara Bio Inc., Kyoto, Japan). We analyzed the messenger RNA (mRNA) levels of Fas by reverse-transcription PCR, as previously reported, using Fas forward primer 5′-GGGCATCTGGACCCTCCTA-3′ and Fas reverse primer 5′- GGCATTAACACTTTTGGACGATAA-3′.

Statistical Analysis. mRNA expression levels of Fas and interferon-stimulated genes (ISGs) were compared using Mann-Whitney's U test and unpaired *t* tests. A *P* value less than 0.05 was considered statistically significant.

Results

Establishment of an Animal Model of Fulminant Hepatitis Using HBV-Infected Human Hepatocyte Chimeric Mice and Human PBMC Transplantation. Administration of 2×10^7 PBMCs twice after suppression of mice NK cells by anti–asialo GM1 antibody[21] and macrophages and DCs by liposome-encapsulated clodronate[22] before transplantation

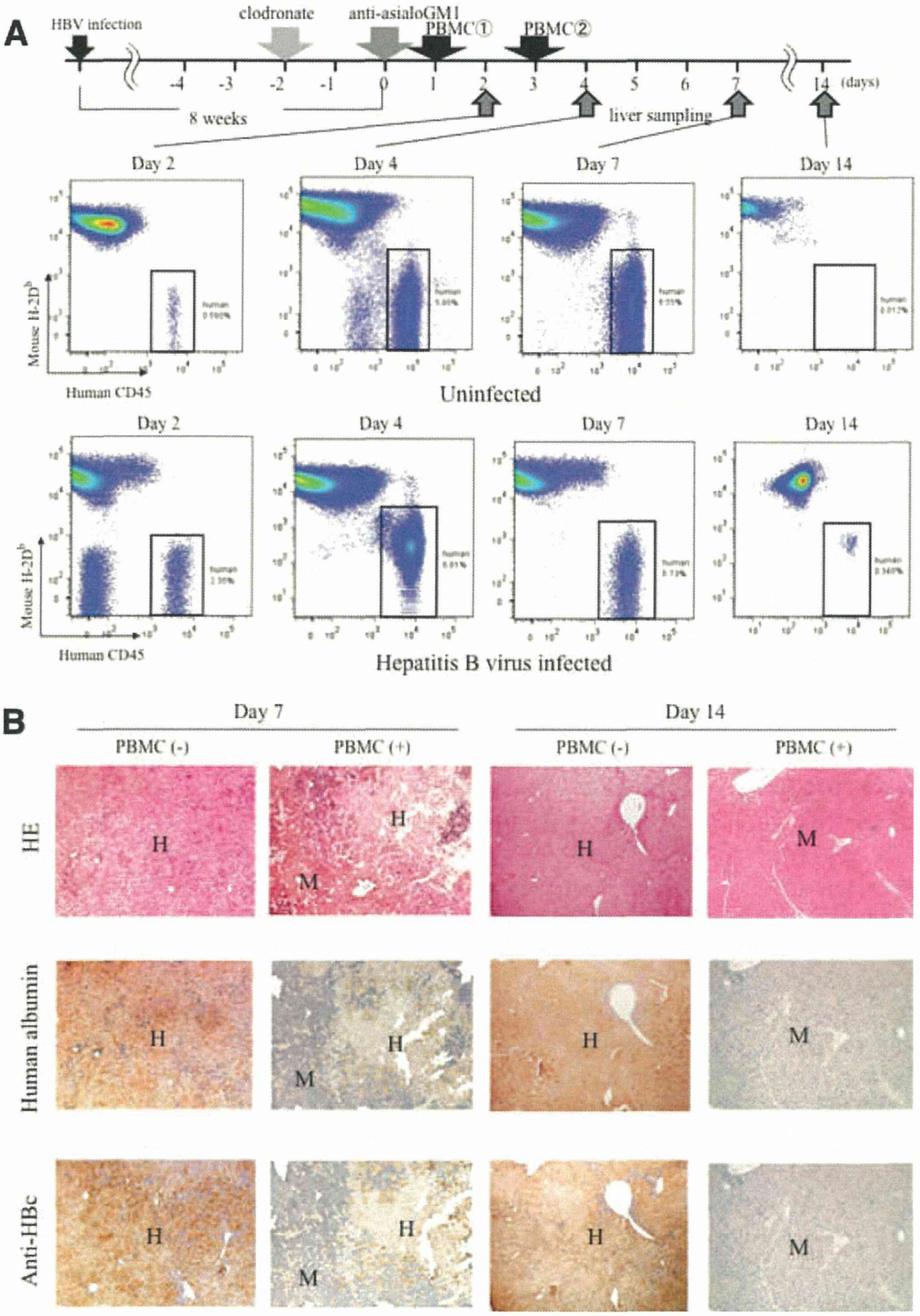

Fig. 1. Establishment of human PBMC chimerism in human hepatocyte chimeric mice. (A) Experimental protocol to establish chimerism and liver sampling is shown at the top of the figure (see Materials and Methods). Scheduling of administration of HBV-positive serum, clodronate, and anti-asialo GM1 antibody and liver sampling by scarification are shown by arrows. Liver mononuclear cells isolated from uninfected (upper panel) and HBV-infected (lower panel) human hepatocyte chimeric mice transplanted with human PBMCs were separated with antibodies for human CD45 and mouse H-2D^b and were analyzed by flow cytometry. Percentage of human mononuclear cells is shown in each panel. Representative figures of two experiments with similar results are shown. (B) Histological analysis of livers of HBV-infected mice. Liver samples obtained from mice with or without human PBMCs at weeks 9 (day 7) and 10 (day 14) were stained with hematoxylin and eosin staining (HE), anti-human albumin antibody, or anti-hepatitis B core antibody. Regions are shown as human (H) and mouse (M) hepatocytes, respectively (original magnification, 40×). (C) Time course of human albumin concentration (upper panel) and HBV DNA titer (lower panel) in mouse serum. Time course of 4 HBV-infected mice transplanted with human PBMCs, 3 HBV-infected mice without human PBMC transplantation, and 4 uninfected mice transplanted with human PBMC are shown. (D) Time course of human albumin concentration (upper panel) and HBV DNA titer (lower panel) in mice. Mice with or without HBV-infection were transplanted with PBMCs obtained from 3 healthy donors who were not vaccinated against hepatitis B.

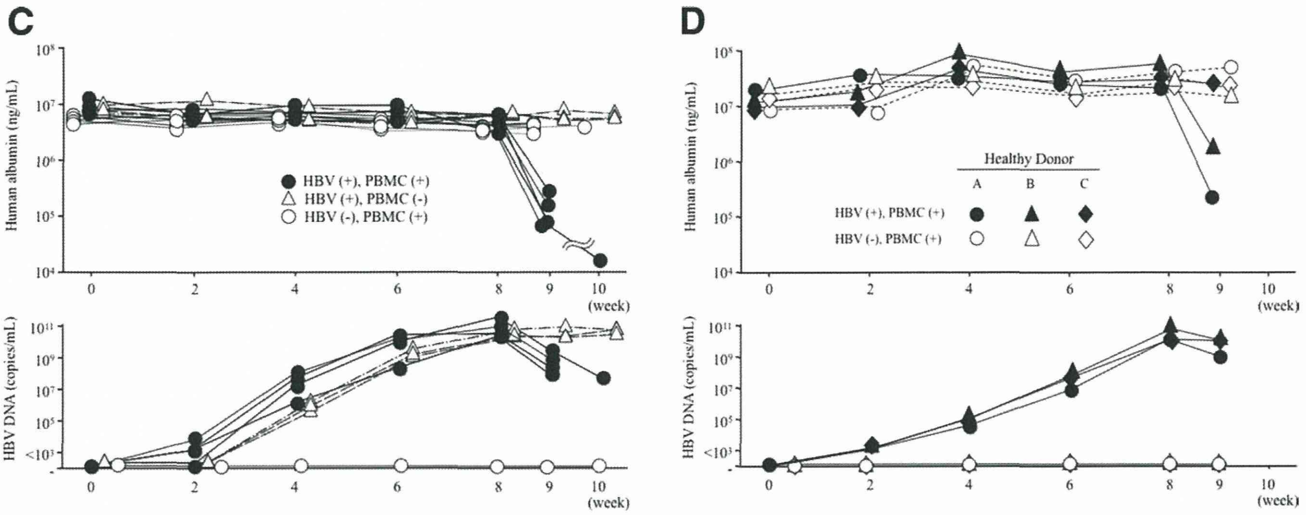

Fig. 1.

enabled us to establish a human PBMC chimerism in uPA-SCID mice. We observed an up to 7% human mononuclear cell chimerism among the liver-resident mononuclear cells of uninfected and HBV-infected mice 2-14 days after the initial injection of PBMC (Fig. 1A; Table 1). Chimerism was most prominent 4 days after initial PBMC administration and almost undetectable by day 14 (Fig. 1A). Histological examination of chimeric mice livers showed extensive human liver cell death, comparable to the massive liver cell death observed in fulminant hepatitis, only in HBV-infected and PBMC-treated mice liver (Fig. 1B). Human hepatocytes were almost completely eliminated and replaced by human albumin-negative mouse hepatocytes at days 7 and 14. Consistent with these histological changes, we observed a rapid decline of HSA levels and HBV DNA only in HBV-infected and PBMC-treated mice (Fig. 1C). The decline of mice HSA levels and HBV DNA was also observed in 2 of 3 HBV-infected mice transplanted with PBMCs isolated from healthy blood donors without HBsAg vaccination (Fig. 1D and Supporting Fig. 2).

Analysis of Liver-Infiltrating Human Lymphocytes Necessary to Establish Massive Hepatocyte Degeneration. We then analyzed liver-infiltrating cells with flow cytometry. Unexpectedly, we did not detect CD8-positive and tetramer-positive CTLs, as reported previously (Fig. 2A). Instead, we observed substantial numbers of CD3-negative and CD56-positive NK cells (Fig. 2B) and small numbers of pDCs and mDCs (Fig. 2C). The majority of NK cells of HBV-infected mice were FasL positive (Fig. 2D). In contrast, such FasL-positive NK cells were not detected in uninfected

Table 1. Analysis of Liver-Infiltrating Cells by Flow Cytometry

	HBV Infected				Uninfected			
Day	No.	Chimerism (%)	Human NK (%)	Fas (+) NK (%)	No.	Chimerism (%)	Human NK (%)	FasL (+) NK (%)
2	1	1.77	2.51	0	1	0.59	12.8	0
	2	2.35	3.02	0.143	2	0.774	58.8	1.1
4	3	6.81	30.7	80.1	3	5.95	42.7	0.678
	4	1.08	68.7	94.7	4	7.11	4.98	0.027
	5	6.60	23.2	58.7	5	5.02	23.1	0.314
7	6	6.73	13.2	0.383	6	6.55	42.1	0.103
	7	5.70	12.5	2.01	7	1.24	13.6	0.025
	8	1.46	3.83	0	8	2.04	1.49	4.03
14	9	0.34	ND	ND	9	0.012	ND	ND
	10	NA*	NA	NA	10	0.013	ND	ND
DCs depleted day 4	11	4.77	5	2.14	11	3.32	4.21	0.465
(by clodronate)	12	1.27	39.5	2.3	12	12.9	9.06	0
DCs depleted day 7	13	2.42	24.8	2.19	13	6.31	54.1	0.131
(by clodronate)	14	1.41	10.6	0.103	14	4.69	1.68	0.12

Abbreviations: NA, not analyzed; ND, not detectable.
*Mouse died just before liver analysis.

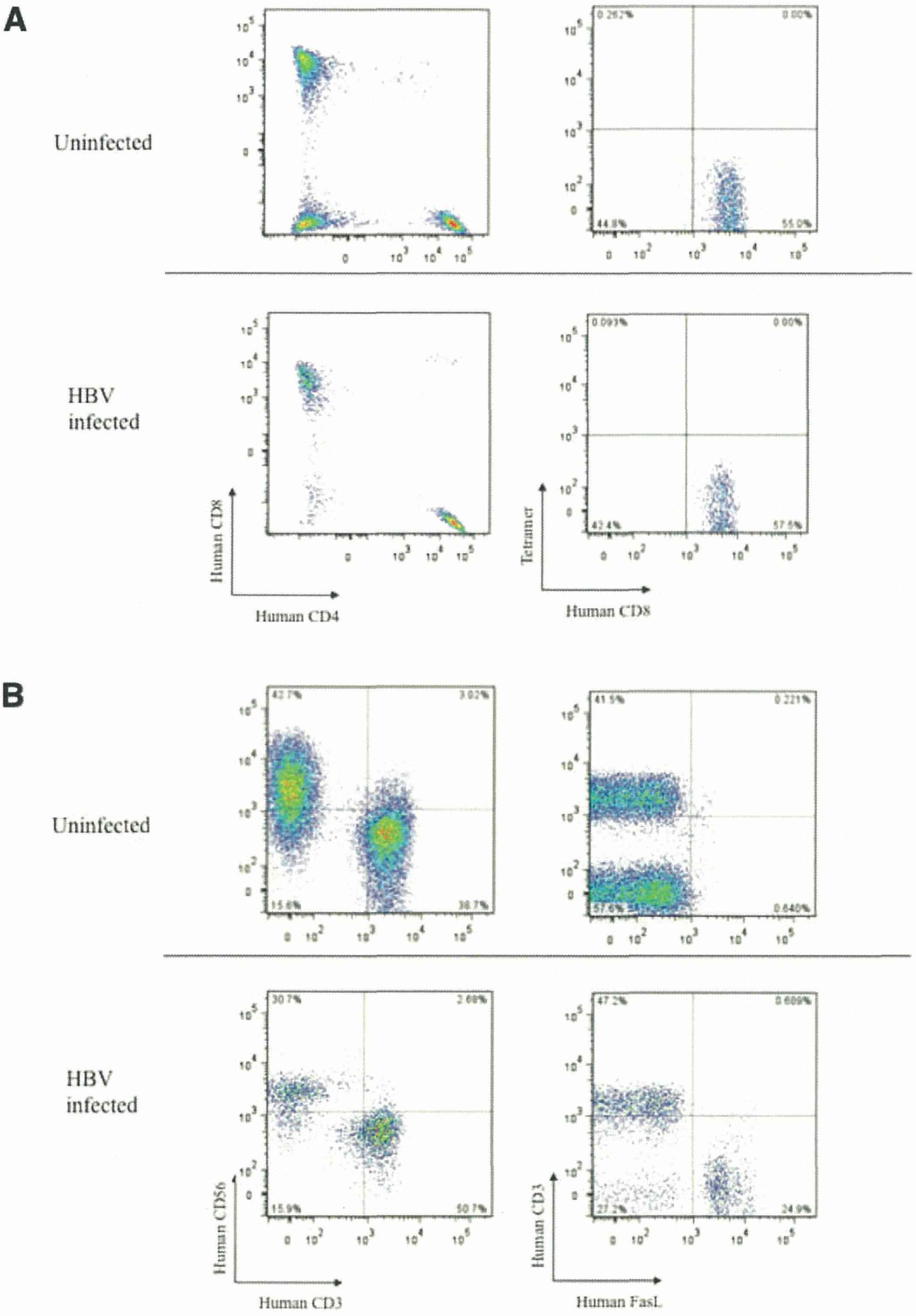

Fig. 2. Analysis of mononuclear cells isolated from day 4 chimeric mouse livers. After defining human PBMCs as mouse H-2Db-human CD45$^+$ cells, we further analyzed the phenotypes of these cells. (A-C) Liver mononuclear cells of uninfected (upper panel) and HBV-infected (lower panel) mice transplanted with human PBMCs were separated with anti-human CD4 and CD8 antibody or anti-human CD8 and HLA-A2 HBcAg tetramer (A), anti-human CD3and CD56 or human CD3 and FasL (B), and anti-human HLA-DR and CD123 and HLA-DR and CD11c (C). (D) Frequency of FasL-positive cells in NK cells were analyzed in uninfected and HBV-infected mice. All figures are representative of two experiments with similar results.

mice livers (Table 1; Fig. 2D), suggesting that these NK cells were activated in HBV-infected mice. These activated NK cells and DCs were detectable in mice livers only 4 days after the initial PBMC injection, but were undetectable after 2 and 7 days (Supporting Figs. 3 and 4, respectively).

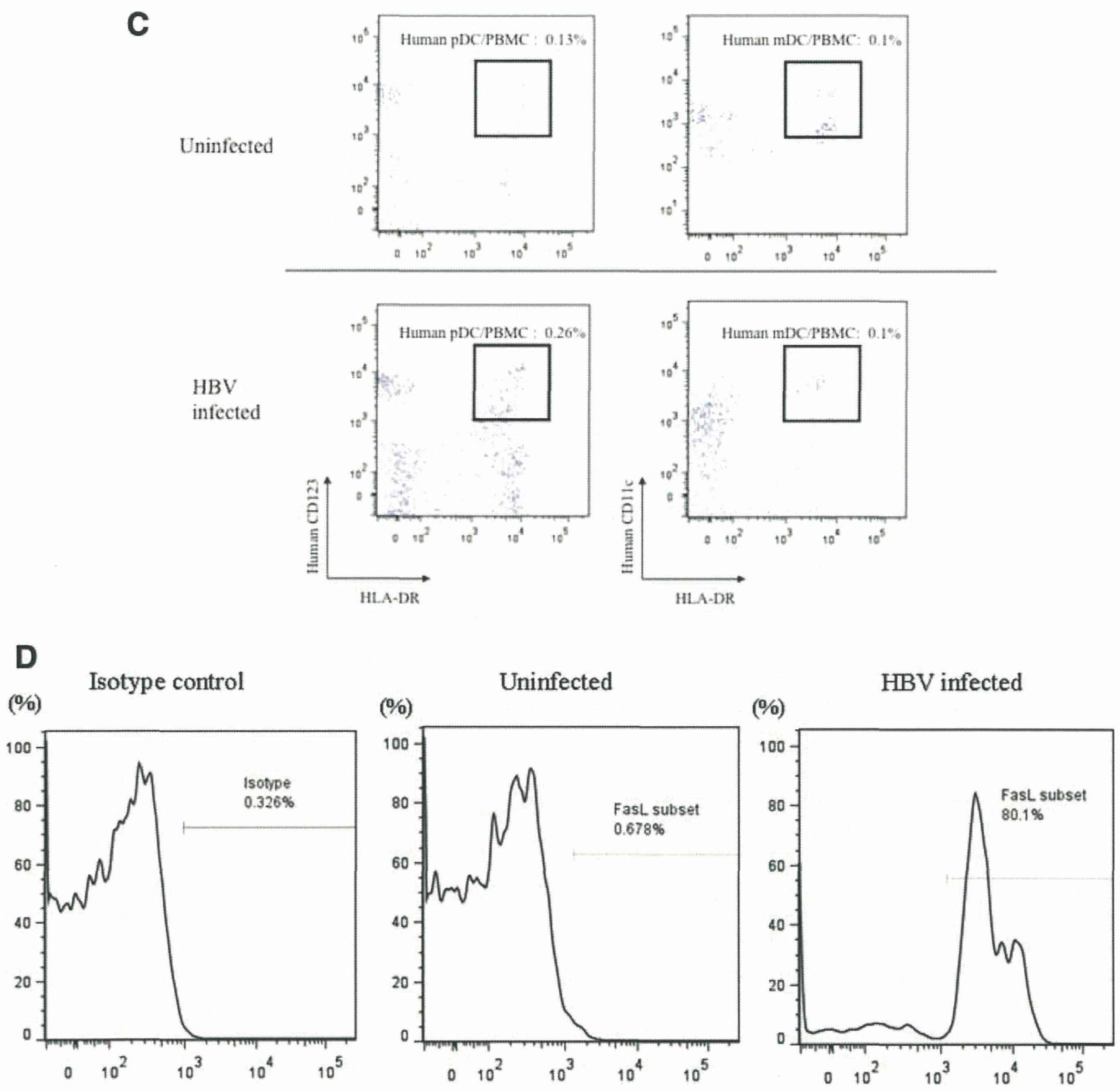

Fig. 2.

Effect of DC Depletion on Establishment of Massive Hepatocyte Degeneration. To confirm the necessity of both DCs and NK cells to complete hepatocyte destruction, we depleted DCs or NK cells with negative selection using antibody-coated magnetic beads before the administration of PBMC. Depletion of either DCs or NK cells completely abolished the decline of human albumin as well as HBV DNA (Supporting Fig. 5A). However, analysis of liver-infiltrating cells revealed that chimerism with human PBMC was poorly established in these animals, probably the result of the loss or damage of human cells by bound antibodies during separation and/or subsequent incubation in mice (Supporting Fig. 5B; Supporting Table 1).

To overcome possible confounding resulting from poor chimerism resulting in poor human hepatocyte degeneration in mice, we attempted to remove DCs from transplanted human PBMCs by alternate means. We attempted to deplete human DCs by administering clodronate 1 day before PBMC transplantation, because we thought that clodronate remaining in the mouse body would impair transplanted human DCs. As expected, we observed an almost complete elimination of DCs by this procedure without impairing

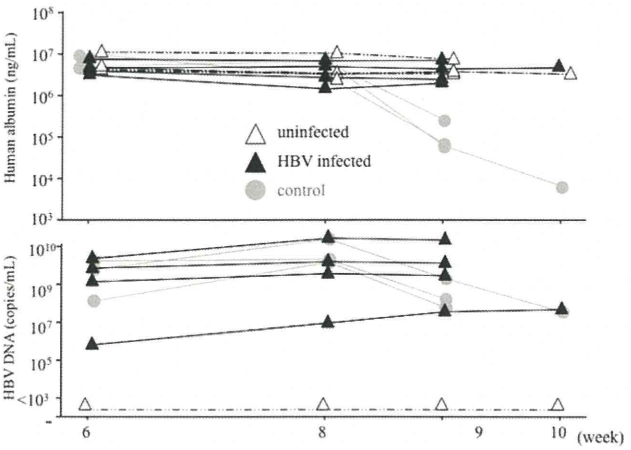

Fig. 3. Time course of mice transplanted with human PBMCs with DC depletion by clodronate 1 day before transplantation. Mice were treated with IP administration of clodronate 1 day before human PBMC transplantation. Time courses of human albumin concentration (upper panel) and HBV DNA titer (lower panel) in mouse serum are shown. Open and closed triangles correspond to 3 uninfected and 4 HBV-infected mice, respectively. Time courses of 3 mice infected with HBV and transplanted with human PBMC 3 days before transplantation (see Fig. 1C) are shown for comparison (shaded closed circle).

PBMC chimerism (Supporting Figs. 6A and 7A; Supporting Table 1). Activation of NK cells was not observed in this setting (Supporting Figs. 6B and 7B; Supporting Table 1). Depletion of DCs completely abolished the decline of both human albumin and HBV DNA (Fig. 3). Histological examination showed that hepatocyte degeneration was absent, and that there were no TUNEL-staining–positive cells (data not shown). Clodronate lyposomes may also nonspecifically deplete macrophages and monocytes in addition to DCs, but no monocytes or macrophages were observed when transplanted PBMCs were analyzed using Ficoll-Hypaque density gradient centrifugation, indicating that the clodronate administration was specifically associated with DC depletion in this study.

Analysis of Fas/FasL System in Massive HBV-Infected Hepatocyte Degeneration Model. We then assessed the importance of the Fas/FasL system and the occurrence of apoptosis in NK-cell–mediated human hepatocyte degeneration. Only HBV-infected human hepatocytes positive for HSA were positive for Fas antibody staining (Fig. 4A). TUNEL staining was also positive only in mice infected with HBV and inoculated with PBMCs (days 4 and 7). Measurement of mRNA levels in infected and uninfected livers showed that expression levels of Fas mRNA increased significantly upon HBV infection (Fig. 4B). To confirm that apoptosis of human hepatocytes was mediated by the Fas/FasL pathway and to determine whether IFN-α or IFN-γ played a role in the establishment of liver cell degeneration, we administered a blocking mAb against FasL, IFN-α, and IFN-γ 1 day before PBMC transplantation. Treatment of mice with antibody against FasL before PBMC completely abolished the decline of human albumin and HBV DNA (Fig. 5A). This abolishment of human albumin decline in mouse serum suggests that the Fas/FasL pathway almost exclusively eliminated infected hepatocytes in this model, which also suggests that Fas-mediated apoptosis could play an important role in FHB. Antibodies against IFN-α and IFN-γ inhibited IFN-induced ISG expression in mice livers (Supporting Fig. 8); however, these antibodies did not disturb the decline of HSA levels (Fig. 5A) and histological inflammation (Fig. 5B). Contact-dependent and -independent activation of NK cells by DCs has been reported previously.[23-25] Although IFN-α and IFN-γ play a role in their activation,[23,25,26] our results indicate that the effects of IFN-α are almost negligible in our experiments (Fig. 5A), suggesting that direct contact among these cells, or cytokines other than IFN-α and IFN-γ, are necessary to activate NK cells in this setting. NK cells have also been reported to exert antiviral effects by secreting IFN-γ. However, our results suggest that this mechanism does not work well in our model (Fig. 5A).

Discussion

In this study, we established a small animal model in which massive hepatocyte degeneration similar to FHB in humans is observed. Our initial attempts to detect human PBMCs in blood or any organ in transplanted mice failed even after injecting 2 × 10^7 cells, which is sufficient to establish human PBMC chimerism in SCID mice.[27] We assumed that failure to develop chimerism was the result of the activity of NK cells and macrophages because the activity of these cells in uPA-SCID mice is higher than in SCID mice.[28,29] Therefore, we attempted to eliminate these effects by administering clodronate and anti–asialo GM1 antibody, which are known to effectively eliminate these cells.[30,31] This assumption appears to be valid, because we were able to establish human PBMC chimerism and massive hepatocyte degeneration by suppressing these cells (Fig. 1).

HBV-specific CTLs have been reported to play an important role in eliminating the virus.[32-34] Accordingly, we attempted to detect HBV-specific CTLs in mice with massive hepatocyte degeneration. Unexpectedly, we failed to detect HBV-specific CTLs (Fig. 2A and Supporting Fig. 9) and instead found that infiltrating cells in the liver were CD3-negative NK cells

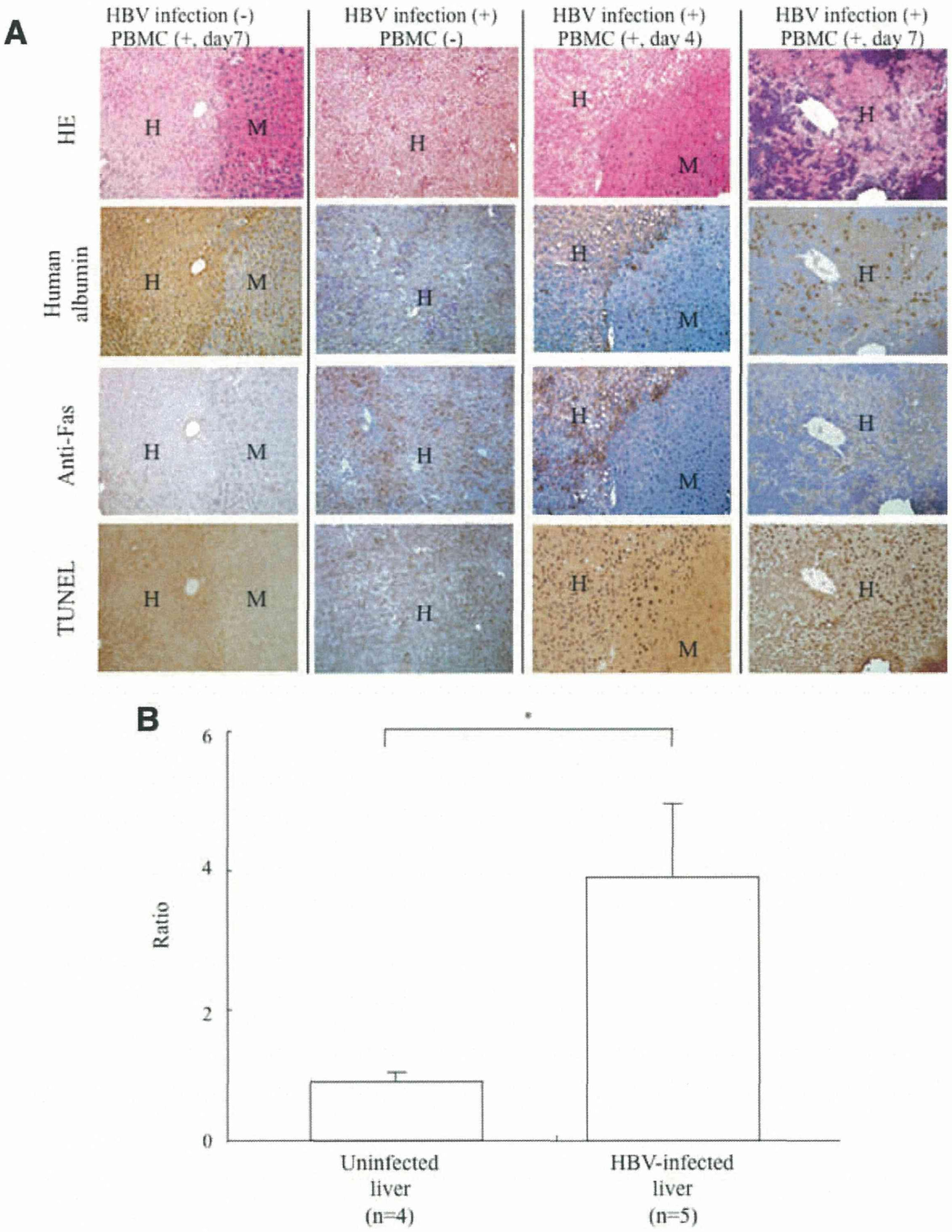

Fig. 4. Assessment of Fas expression in the liver in human hepatocyte chimeric mice. (A) Histological analysis of chimeric mice livers transplanted with human PBMCs but without HBV infection (day 7), with HBV infection but without PBMC transplantation, and with HBV infection and PBMC transplantation at days 4 and 7. Liver samples were stained with hematoxylin and eosin staining (HE), anti-human albumin antibody, anti-human Fas antibody, and TUNEL staining. Regions are shown as human (H) and mouse (M) hepatocytes, respectively (original magnification, 100×). Note that Fas antigen was expressed only in HBV-infected human hepatocytes, and TUNEL staining is only positive for HBV-infected and human PBMC-transplanted mice livers. Mouse hepatocytes were negative for all three stains. (B) Expression of Fas mRNA levels in uninfected and HBV-infected human hepatocytes. Data are represented as mean ± standard deviation. $*P < 0.001$.

(Fig. 2B,D and Supporting Fig. 10). The reason for the absence of CTLs in our experiment is unknown, but this suggests that massive hepatocyte degeneration resembling fulminant hepatitis can be caused by NK cells as a main player, and recent reports demonstrating that NK cells contribute to severe acute and

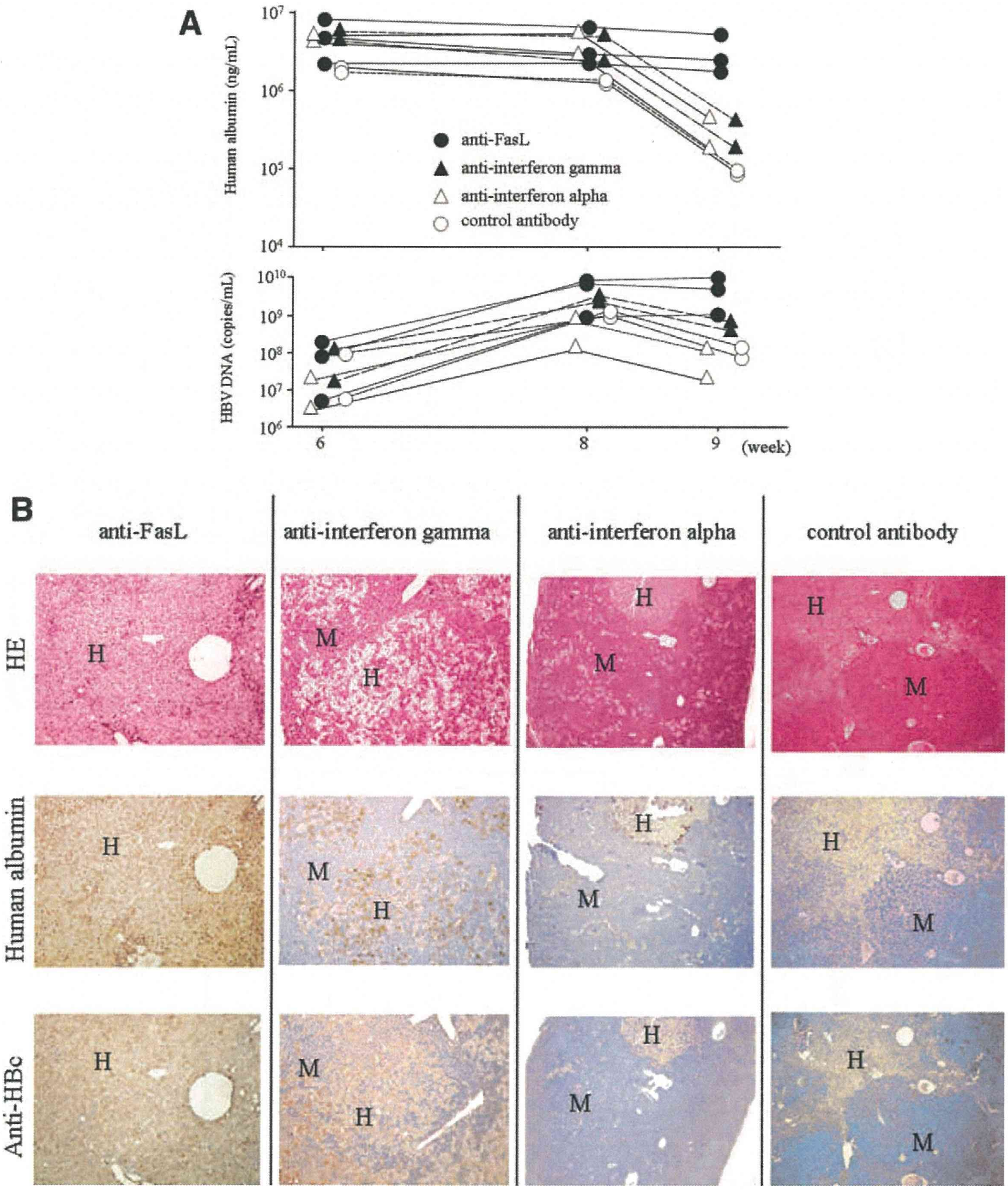

Fig. 5. Effect of anti-FasL, anti-IFN-γ and anti-IFN-α antibody administration on HSA and HBV DNA. (A) Time courses of HSA (upper panel) and HBV DNA (lower panel) before and 1 week after human PBMC transplantation are shown. Mice were pretreated with antibodies against human Fas-L, IFN-γ, and IFN-α before PBMC transplantation, as described in Materials and Methods. Isotype antibody was used as a control. (B) Histological analysis of livers of HBV-infected mice injected with anti-human FasL mAb, IFN-γ, IFN-α, and control antibody. Liver samples obtained from mice with human PBMCs at weeks 9 (day 7) were stained with hematoxylin and eosin staining (HE), antihuman albumin antibody, or antihepatitis B core antibody. Regions are shown as human (H) and mouse (M) hepatocytes, respectively (original magnification, 40×).

chronic hepatitis B (CHB) support this assertion.[11,35] We attempted to collect CTLs from HBV-infected patients and to establish hepatitis in chimeric mice. However, we rarely detected tetramer-positive CTLs in blood samples from chronically infected patients and were therefore unable to establish hepatitis using CD8-positive T cells. Consequently, a limitation of this study is that differential roles of NK cells and CTLs in massive liver cell death could not be examined.

Although it is not clear in this study how profoundly DC and NK cell activity plays a role in patients with FHB, our results suggest that the immune system can trigger severe hepatocyte degeneration. The importance of the activation of NK cells by DCs was evident, because depletion of DCs almost completely abolished the massive hepatocyte degeneration in this model (Supporting Fig. 10; Table 1). The interaction between NK cells and DCs is not well characterized, although it has been established that antigen-presenting accessory cells provide both indirect (i.e., soluble) and direct (i.e., contact-dependent) signals to T cells. Experiments in which NK cells are separated from pathogens and antigen-presenting cells by semipermeable membranes are cultured with supernatants from pathogen-activated DCs or in which cytokines are neutralized with blocking antibodies. These reports indicate that both soluble and contact-dependent signals may contribute to the activation of NK cells.[23,25,26]

The importance of the Fas/FasL system in hepatocyte damage in acute and chronic HBV infection has been reported previously.[37,38] However, the extent to which this system plays a role in human hepatitis B, especially fulminant hepatitis, is unknown. As shown in this study (Fig. 5A), inhibition of the Fas/FasL system by anti-Fas antibody dramatically reduced the effect of human PBMC transplantation. This showed the possibility that the Fas/FasL system plays an important role in the degeneration of infected hepatocytes in FHB. Further studies should be conducted to evaluate what immunological responses play important roles in human hepatitis B.

The importance of NK-cell activity suggests that the suppression of DCs and NK-cell activity or the Fas/FasL system might have therapeutic implications for FHB.[11,35] If DCs and NK-cell activity or Fas/FasL activity could be controlled in the early stages of severe acute or fulminant hepatitis, we might be able to control hepatitis activity and prevent subsequent liver failure. Of course, it would be necessary to monitor the development of chronic hepatitis after such treatment because DCs and NK cells contribute to early host defenses and shape subsequent adaptive immune response through complex cross-talk regulating the early phase of the immune response.[19,24,39,40]

We analyzed liver damage using HBV genotype C–infected mice in this study. However, HBV genotype C is associated with more severe histological liver damage than genotype B,[41] and future studies should compare immunological differences between genotypes B and C.

In summary, we established an animal model of FHB using highly repopulated human hepatocyte chimeric mice and transplanted human PBMCs. Modifications of this model will facilitate further research into acute and CHB using human immune cells, including HBV-directed CTL clones, suppressor and regulatory T cells, as well as immunological experiments to study interactions between DCs and NK cells. Such models may be useful to develop and evaluate new therapeutic strategies against HBV infection.

Acknowledgment: The authors thank Rie Akiyama and Yoko Matsumoto for their expert technical assistance. This work was carried out at the Analysis Center of Life Science, Natural Science Center for Basic Research and Development, Hiroshima University.

References

1. Bernal W, Auzinger G, Dhawan A, Wendon J. Acute liver failure. Lancet 2010;376:190-201.
2. Leifeld L, Cheng S, Ramakers J, Dumoulin FL, Trautwein C, Sauerbruch T, Spengler U. Imbalanced intrahepatic expression of interleukin 12, interferon gamma, and interleukin 10 in fulminant hepatitis B. HEPATOLOGY 2002;36:1001-1008.
3. Ozasa A, Tanaka Y, Orito E, Sugiyama M, Kang JH, Hige S, et al. Influence of genotypes and precore mutations on fulminant or chronic outcome of acute hepatitis B virus infection. HEPATOLOGY 2006;44: 326-334.
4. Kawai T, Akira S. Toll-like receptor and RIG-I-like receptor signaling. Ann N Y Acad Sci 2008;1143:1-20.
5. Maini MK, Boni C, Lee CK, Larrubia JR, Reignat S, Ogg GS, et al. The role of virus-specific CD8(+) cells in liver damage and viral control during persistent hepatitis B virus infection. J Exp Med 2000;191: 1269-1280.
6. Guidotti LG, Ando K, Hobbs MV, Ishikawa T, Runkel L, Schreiber RD, Chisari FV. Cytotoxic T lymphocytes inhibit hepatitis B virus gene expression by a noncytolytic mechanism in transgenic mice. Proc Natl Acad Sci U S A 1994;91:3764-3768.
7. Ando K, Moriyama T, Guidotti LG, Wirth S, Schreiber RD, Schlicht HJ, et al. Mechanisms of class I restricted immunopathology. A transgenic mouse model of fulminant hepatitis. J Exp Med 1993;178: 1541-1554.
8. Cote PJ, Toshkov I, Bellezza C, Ascenzi M, Roneker C, Ann Graham L, et al. Temporal pathogenesis of experimental neonatal woodchuck hepatitis virus infection: increased initial viral load and decreased severity of acute hepatitis during the development of chronic viral infection. HEPATOLOGY 2000;32:807-817.
9. Chisari FV. Rous-Whipple Award Lecture. Viruses, immunity, and cancer: lessons from hepatitis B. Am J Pathol 2000;156:1117-1132.
10. Dunn C, Brunetto M, Reynolds G, Christophides T, Kennedy PT, Lampertico P, et al. Cytokines induced during chronic hepatitis B virus infection promote a pathway for NK cell-mediated liver damage. J Exp Med 2007;204:667-680.
11. Zhang Z, Zhang S, Zou Z, Shi J, Zhao J, Fan R, et al. Hypercytolytic activity of hepatic natural killer cells correlates with liver injury in chronic hepatitis B patients. HEPATOLOGY 2011;53:73-85.
12. Dandri M, Burda MR, Torok E, Pollok JM, Iwanska A, Sommer G, et al. Repopulation of mouse liver with human hepatocytes and *in vivo* infection with hepatitis B virus. HEPATOLOGY 2001;33:981-988.
13. Petersen J, Burda MR, Dandri M, Rogler CE. Transplantation of human hepatocytes in immunodeficient UPA mice: a model for the study of hepatitis B virus. Methods Mol Med 2004;96:253-260.
14. Ogata N, Miller RH, Ishak KG, Purcell RH. The complete nucleotide sequence of a pre-core mutant of hepatitis B virus implicated in fulminant hepatitis and its biological characterization in chimpanzees. Virology 1993;194:263-276.

15. Tateno C, Yoshizane Y, Saito N, Kataoka M, Utoh R, Yamasaki C, et al. Near completely humanized liver in mice shows human-type metabolic responses to drugs. Am J Pathol 2004;165:901-912.
16. Tsuge M, Hiraga N, Takaishi H, Noguchi C, Oga H, Imamura M, et al. Infection of human hepatocyte chimeric mouse with genetically engineered hepatitis B virus. Hepatology 2005;42:1046-1054.
17. Tsuge M, Hiraga N, Akiyama R, Tanaka S, Matsushita M, Mitsui F, et al. HBx protein is indispensable for development of viraemia in human hepatocyte chimeric mice. J Gen Virol 2010;91:1854-1864.
18. Kuhober A, Pudollek HP, Reifenberg K, Chisari FV, Schlicht HJ, Reimann J, Schirmbeck R. DNA immunization induces antibody and cytotoxic T cell responses to hepatitis B core antigen in H-2b mice. J Immunol 1996;156:3687-3695.
19. Banchereau J, Steinman RM. Dendritic cells and the control of immunity. Nature 1998;392:245-252.
20. Shortman K, Liu YJ. Mouse and human dendritic cell subtypes. Nat Rev Immunol 2002;2:151-161.
21. Sandhu J, Shpitz B, Gallinger S, Hozumi N. Human primary immune response in SCID mice engrafted with human peripheral blood lymphocytes. J Immunol 1994;152:3806-3813.
22. Gonzalez SF, Lukacs-Kornek V, Kuligowski MP, Pitcher LA, Degn SE, Kim YA, et al. Capture of influenza by medullary dendritic cells via SIGN-R1 is essential for humoral immunity in draining lymph nodes. Nat Immunol 2010;11:427-434.
23. Fernandez NC, Lozier A, Flament C, Ricciardi-Castagnoli P, Bellet D, Suter M, et al. Dendritic cells directly trigger NK cell functions: cross-talk relevant in innate anti-tumor immune responses *in vivo*. Nat Med 1999;5:405-411.
24. Ferlazzo G, Tsang ML, Moretta L, Melioli G, Steinman RM, Munz C. Human dendritic cells activate resting natural killer (NK) cells and are recognized via the NKp30 receptor by activated NK cells. J Exp Med 2002;195:343-351.
25. Andoniou CE, van Dommelen SL, Voigt V, Andrews DM, Brizard G, Asselin-Paturel C, et al. Interaction between conventional dendritic cells and natural killer cells is integral to the activation of effective antiviral immunity. Nat Immunol 2005;6:1011-1019.
26. Walzer T, Dalod M, Robbins SH, Zitvogel L, Vivier E. Natural-killer cells and dendritic cells: "l'union fait la force". Blood 2005;106: 2252-2258.
27. Mosier DE, Gulizia RJ, Baird SM, Wilson DB, Spector DH, Spector SA. Human immunodeficiency virus infection of human-PBL-SCID mice. Science 1991;251:791-794.
28. Kawahara T, Douglas DN, Lewis J, Lund G, Addison W, Tyrrell DL, et al. Critical role of natural killer cells in the rejection of human hepatocytes after xenotransplantation into immunodeficient mice. Transpl Int 2010;23:934-943.
29. Morosan S, Hez-Deroubaix S, Lunel F, Renia L, Giannini C, Van Rooijen N, et al. Liver-stage development of *Plasmodium falciparum*, in a humanized mouse model. J Infect Dis 2006;193:996-1004.
30. Dorshkind K, Pollack SB, Bosma MJ, Phillips RA. Natural killer (NK) cells are present in mice with severe combined immunodeficiency (SCID). J Immunol 1985;134:3798-3801.
31. Ito M, Hiramatsu H, Kobayashi K, Suzue K, Kawahata M, Hioki K, et al. NOD/SCID/gamma(c)(null) mouse: an excellent recipient mouse model for engraftment of human cells. Blood 2002;100:3175-3182.
32. Thimme R, Wieland S, Steiger C, Ghrayeb J, Reimann KA, Purcell RH, Chisari FV. CD8(+) T cells mediate viral clearance and disease pathogenesis during acute hepatitis B virus infection. J Virol 2003;77: 68-76.
33. Rehermann B, Fowler P, Sidney J, Person J, Redeker A, Brown M, et al. The cytotoxic T lymphocyte response to multiple hepatitis B virus polymerase epitopes during and after acute viral hepatitis. J Exp Med 1995;181:1047-1058.
34. Webster GJ, Reignat S, Maini MK, Whalley SA, Ogg GS, King A, et al. Incubation phase of acute hepatitis B in man: dynamic of cellular immune mechanisms. Hepatology 2000;32:1117-1124.
35. Zou Y, Chen T, Han M, Wang H, Yan W, Song G, et al. Increased killing of liver NK cells by Fas/Fas ligand and NKG2D/NKG2D ligand contributes to hepatocyte necrosis in virus-induced liver failure. J Immunol 2010;184:466-475.
36. Newman KC, Riley EM. Whatever turns you on: accessory-cell-dependent activation of NK cells by pathogens. Nat Rev Immunol 2007; 7:279-291.
37. Galle PR, Hofmann WJ, Walczak H, Schaller H, Otto G, Stremmel W, et al. Involvement of the CD95 (APO-1/Fas) receptor and ligand in liver damage. J Exp Med 1995;182:1223-1230.
38. Rivero M, Crespo J, Fábrega E, Casafont F, Mayorga M, Gomez-Fleitas M, Pons-Romero F. Apoptosis mediated by the Fas system in the fulminant hepatitis by hepatitis B virus. J Viral Hepat 2002;9: 107-113.
39. Moretta A. Natural killer cells and dendritic cells: rendezvous in abused tissues. Nat Rev Immunol 2002;2:957-964.
40. Asselin-Paturel C, Trinchieri G. Production of type I interferons: plasmacytoid dendritic cells and beyond. J Exp Med 2005;202:461-465.
41. Orito E, Ichida T, Sakugawa H, Sata M, Horiike N, Hino K, et al. Geographic distribution of hepatitis B virus (HBV) genotype in patients with chronic HBV infection in Japan. Hepatology 2001;34: 590-594.

Hepatitis B Virus-Specific miRNAs and Argonaute2 Play a Role in the Viral Life Cycle

C. Nelson Hayes[1,2,3⑨], **Sakura Akamatsu**[1,2,3⑨], **Masataka Tsuge**[3,4], **Daiki Miki**[1,2,3], **Rie Akiyama**[1,2,3], **Hiromi Abe**[1,2], **Hidenori Ochi**[1,2,3], **Nobuhiko Hiraga**[1,2,3], **Michio Imamura**[1,2,3], **Shoichi Takahashi**[1,2], **Hiroshi Aikata**[1,3], **Tomokazu Kawaoka**[1,2,3], **Yoshiiku Kawakami**[1,2,3], **Waka Ohishi**[3,5], **Kazuaki Chayama**[1,2,3*]

1 Department of Gastroenterology and Metabolism, Applied Life Sciences, Institute of Biomedical & Health Sciences, Hiroshima University, Hiroshima, Japan, **2** Laboratory for Digestive Diseases, Center for Genomic Medicine, RIKEN, Hiroshima, Japan, **3** Liver Research Project Center, Hiroshima University, Hiroshima, Japan, **4** Natural Science Center for Basic Research and Development, Hiroshima University, Hiroshima, Japan, **5** Department of Clinical Studies, Radiation Effects Research Foundation, Hiroshima, Japan

Abstract

Disease-specific serum miRNA profiles may serve as biomarkers and might reveal potential new avenues for therapy. An HBV-specific serum miRNA profile associated with HBV surface antigen (HBsAg) particles has recently been reported, and AGO2 and miRNAs have been shown to be stably associated with HBsAg in serum. We identified HBV-associated serum miRNAs using the Toray 3D array system in 10 healthy controls and 10 patients with chronic hepatitis B virus (HBV) infection. 19 selected miRNAs were then measured by quantitative RT-PCR in 248 chronic HBV patients and 22 healthy controls. MiRNA expression in serum versus liver tissue was also compared using biopsy samples. To examine the role of AGO2 during the HBV life cycle, we analyzed intracellular co-localization of AGO2 and HBV core (HBcAg) and surface (HBsAg) antigens using immunocytochemistry and proximity ligation assays in stably transfected HepG2 cells. The effect of AGO2 ablation on viral replication was assessed using siRNA. Several miRNAs, including miR-122, miR-22, and miR-99a, were up-regulated at least 1.5 fold ($P<2E-08$) in serum of HBV-infected patients. AGO2 and HBcAg were found to physically interact and co-localize in the ER and other subcellular compartments. HBs was also found to co-localize with AGO2 and was detected in multiple subcellular compartments. Conversely, HBx localized non-specifically in the nucleus and cytoplasm, and no interaction between AGO2 and HBx was detected. SiRNA ablation of AGO2 suppressed production of HBV DNA and HBs antigen in the supernatant.

Conclusion: These results suggest that AGO2 and HBV-specific miRNAs might play a role in the HBV life cycle.

Citation: Hayes CN, Akamatsu S, Tsuge M, Miki D, Akiyama R, et al. (2012) Hepatitis B Virus-Specific miRNAs and Argonaute2 Play a Role in the Viral Life Cycle. PLoS ONE 7(10): e47490. doi:10.1371/journal.pone.0047490

Editor: Sang-Hoon Ahn, Yonsei University College of Medicine, Republic of Korea

Received July 2, 2012; **Accepted** September 11, 2012; **Published** October 16, 2012

Funding: This work was supported in part by Grants-in-Aid for scientific research and development from the Ministry of Health, Labor and Welfare and Ministry of Education Culture Sports Science and Technology, Government of Japan. The funders had no role in study design, data collection and analysis, decision to publish, or preparation of the manuscript.

Competing Interests: The authors have declared that no competing interests exist.

* E-mail: chayama@hiroshima-u.ac.jp

⑨ These authors contributed equally to this work.

Introduction

Hepatitis B virus (HBV) is a partially double-stranded DNA virus in the Hepadnaviridae family [1]. New therapies are urgently needed for the 350 million chronically infected individuals who face a significantly elevated lifetime risk of cirrhosis and hepatocellular carcinoma [2,3]. Recent insight into the role of non-coding RNAs in the liver has highlighted potential applications of microRNAs (miRNAs) in HBV diagnosis and treatment [4,5,6,7,8,9].

MiRNAs are a class of short non-coding RNAs involved in post-transcriptional gene regulation of multiple pathways [10]. In contrast to messenger RNAs, exosome-free extracellular miRNAs may be nuclease-resistant and remain in circulation for long periods of time by being stably bound to AGO2, a component of the RNA-induced silencing complex [11]. The origin and function of these extracellular miRNAs is unclear, but they may serve as biomarkers for liver injury and cancer [4]. Elucidating the function of hepatic miRNAs in HBV infection is important in the development of strategies to eradicate the virus and assess the risk of HCC. A number of miRNAs have been shown to be up- or down-regulated in HBV infection [4,12,13]. Noting that the defective hepatitis delta virus co-opts HBsAg subviral particles for export, Novellino et al. hypothesized that HBsAg subviral particles might also sequester miRNAs from the liver [5]. Using HBsAg immunoprecipitation, they identified a set of liver-specific and immune regulatory AGO2-bound miRNAs associated with HBsAg.

These reports suggest that AGO2 and a specific subset of miRNAs may participate in HBV replication, either as part of a host anti-HBV defense or as viral strategy to exploit or evade the RISC machinery. In this study, we examined serum miRNA expression in chronic HBV and healthy individuals and found a specific subset of miRNAs that are over-expressed in HBV-positive patients and in which miR-122 was strongly up-regulated. To determine whether components of the miRNA system are associated with other HBV components, we performed subcellular localization experiments with viral proteins and AGO2.

Materials and Methods

Study Subjects

We performed a series of experiments to compare miRNA profiles of healthy and HBV-infected individuals in serum and liver tissue. All patients had chronic hepatitis B and agreed to provide blood samples for a viral hepatitis study. Patient profiles are shown in Table 1. Histopathological diagnosis was made according to the criteria of Desmet et al. [14]. The study protocol conforms to the ethical guidelines of the 1975 Declaration of Helsinki, and all patients provided written informed consent. This study was approved a priori by the ethical committee of Hiroshima University.

miRNA Expression Levels in Serum

miRNA expression in serum samples was measured using the Toray Industries miRNA analysis system, in which serum miRNA samples were hybridized to 3D-Gene human miRNA ver12.1 chips containing 900 miRNAs (Toray Industries, Inc., Tokyo, Japan). MiRNA gene expression data were scaled by global normalization, and differential expression was analyzed using the limma package in the R statistical framework. Serum was collected from 20 patients with high HBV DNA and HBsAg levels and with either high (>42 IU/l) or low (≤42 IU/l) ALT levels. Serum from the 10 low ALT patients was analyzed as a mixture, whereas serum from each of the 10 high ALT patients was analyzed both separately and as a mixture. For comparison with healthy controls we collected separate mixtures of serum from 10 healthy females and 12 healthy males. Serum samples from each healthy female were also measured separately. All healthy controls were negative for HBsAg, HBcAb, and HCV Ab. For comparison with miRNA expression in hepatocytes, miRNA expression was measured in non-tumor biopsy tissue from an HBV-infected patient and compared to non-cancerous liver tissue samples from two patients without HBV or HCV infection.

Table 1. Clinical characteristics of chronic hepatitis B virus patients (n = 248).

Factor	Value
Age	44 (15–76)
Sex (male/female)	169/77
Alanine aminotransferase (IU/l)	56 (10–1867)
Aspartate aminotransferase (IU/l)	43.5 (15–982)
HBV DNA (IU/ml)	6.3 (1.8–9.1)
Liver fibrosis (1/2/3/4)	69/102/46/26
Necroinflammatory activity (0/1/2/3/4)	1/70/127/45/0
γ-glutamyl transpeptidase (IU/l)	43 (9–459)
Alpha-fetoprotein (μg/l)	6.15 (0–9400)
Promthrombin time (s)	93 (0–146)
Albumin (g/dl)	4.4 (0–5.2)
Platelets (x10^4/mm^3)	16.75 (1–36)
HBsAg (IU/l)	2765 (0.05–239000)
HBeAg (−/+)	115/127
HBeAb (−/+)	113/128

Continuous variables are shown as median and range, and categorical variables are shown as counts.

Fibrosis and necroinflammatory activity were scored according to the criteria of Desmet et al. [14].

doi:10.1371/journal.pone.0047490.t001

Quantitative Real-time Polymerase Chain Reaction miRNA Analysis

Using real-time polymerase chain reaction (RT-PCR) we measured the expression of 19 miRNAs in serum from 248 patients with chronic HBV infection and from 10 healthy females and 12 healthy males. Circulating microRNA was extracted from 300 μl of serum samples using the mirVana PARIS Kit (Ambion, Austin, TX) according to the manufacturer's instructions. RNA was eluted in 80 μl of nuclease free water and reverse transcribed using TaqMan MicroRNA Reverse Transcription Kit (Life Technologies Japan, Tokyo, Japan). *Caenorhabditis elegans* miR-238 (cel-miR-238) was spiked to each sample as a control for extraction and amplification steps. The reaction mixture contained 5 μl of RNA solution, 2 μl of 10× reverse transcription buffer, 0.2 μl of 100 mM dNTP mixture, 4 μl of 5× RT primer, 0.25 μl of RNase inhibitor and 7.22 μl of nuclease free water in a total volume of 20 μl. The reaction was performed at 16°C for 30 min followed by 42°C for 30 min. The reaction was terminated by heating the solution at 85°C for 5 min. MiRNAs were amplified using primers and probes provided by Applied Biosystems using TaqMan MicroRNA assays according to the manufacturer's instructions. The reaction mixture contained 12.5 μl of 2× Universal PCR Master Mix, 1.25 μl of 20× TaqMan Assay solution, 1 μl of reverse transcription product and 10.25 μl of nuclease free water in a total volume of 25 μl. Amplification conditions were 95°C for 10 min followed by 50 denaturing cycles for 15 sec at 95°C and annealing and extension for 60 sec at 60°C in an ABI7300 thermal cycler. For the cel-miR-238 assay, a dilution series using chemically synthesized miRNA was used to generate a standard curve that permitted absolute quantification of molecules.

Pathway Analysis

Target genes of differentially expressed miRNAs were predicted based on agreement among three miRNA prediction tools, miRanda, miRBase, and TargetScan. Gene Set Enrichment Analysis (http://www.broadinstitute.org/gsea) was used to identify significantly over-represented gene ontology (GO) terms among the predicted targets.

Plasmid Construction

The construction of wild-type HBV 1.4 genome length, pTRE-HB-wt, was described previously [15]. We used pTRE2 vector without pTet-off vector and doxycycline because a sufficient amount of HBV transcript was produced from internal HBV promoters, and transcription from the pTRE2 promoter is negligible under these conditions. The nucleotide sequence of the HBV genome that we cloned into plasmids pTRE-HB-wt was deposited into GenBank under accession number AB206817.

Cell Culture

HepG2 cells, derived from a human hepatoma cell line, were grown in Dulbecco's modified Eagle's medium (DMEM) supplemented with 10% (v/v) fetal bovine serum at 37°C and under 5% CO_2. For the production of stably transfected cell lines, HepG2 cells were transfected with 20μg of the plasmid pTRE-HB-wt by calcium precipitation and the transfected cells were selected with

400µg/ml hygromycin-included DMEM. Sixty colonies were isolated, and clones that were positive for both HBs and HBe antigens were selected. Finally, one cell line named T23 was selected and used for further experiments. T23 cells continuously produced more than 6 log copies/ml of HBV DNA in supernatant over more than 12 months (data not shown).

Immunocytochemistry

Co-localization between AGO2 and several HBV proteins (HBc, HBs, and HBx) was analyzed using immunocytochemistry, followed by cellular localization assays using antibodies targeting various sub-cellular compartments. HepG2 or T23 cells were seeded in 2-well chamber plates and harvested 48 hours after seeding. The cells were washed with PBS and fixed with 4% (v/v) paraformaldehyde. After fixation, the cells were stained with several primary antibodies (Table S1). The bound antibodies were detected with an Alexa 488-conjugated antibody against rabbit IgG (1:2000) or Alexa 568-conjugated antibody against mouse IgG (1:2000), respectively (Molecular Probes, Eugene, OR). Nuclei were counterstained with 6-diamidino-2-phenylindole (DAPI) (Vector laboratories, Burlingame, CA). The stained cells were examined with a Fluoview FV10i microscope (Olympus, Tokyo, Japan).

In situ Proximity Ligation Assay

We used proximity ligation assays (PLA) to determine whether AGO2 and HBc physically interact. PLA is a recent method to detect protein-protein interactions using protein-DNA conjugates that can be detected using fluorescence microscopy [16]. PLA improves on traditional immunoassays by directly detecting even weak or transient protein interactions [16]. HepG2 and T23 cells were seeded in 2-well chamber plates and harvested 48 hours after seeding. The cells were washed with PBS and fixed with 4% (v/v) paraformaldehyde. After fixation, the cells were stained with primary antibodies. The primary antibodies used are listed in Table S1. After overnight incubation with primary antibody at 4°C, PLA was performed using Duolink II PLA probe anti-rabbit plus and anti-mouse minus and Duolink II Detection Reagents Orange (Olink, Uppsala, Sweden) following the manufacturer's protocol. Nuclei were counterstained with DAPI. Imaging was performed using a Fluoview FV10i microscope.

Analysis of Supernatant HBV Production by RNA Interference Against AGO2

To investigate the necessity of AGO2 for HBV production, we performed RNA interference assay using T23 cells that are HepG2 cells stably transfected with the plasmid pTRE-HB-wt. We used Silencer Select Pre-designed siRNA small interfering RNA targeting *AGO2* (#s25932, Ambion, Austin, TX) and Silencer Select Negative Control #1 siRNA for control (Ambion). T23 cells were transfected with one of the siRNA oligonucleotides (10 nM) using Lipofectamine RNAiMAX (Invitrogen, Carlsbad, CA) according to the manufacturer's instructions. To examine the knockdown effect of siRNAs against *AGO2* by real-time quantitative RT-PCR, T23 cells transfected with siRNAs were harvested 72 hours after transfection. Total RNA was isolated using the QuickGene RNA cultured cell kit S (Fujifilm, Tokyo, Japan). One µg of each RNA sample was reverse transcribed with the SuperScript VILO cDNA Synthesis kit (Invitrogen). First-strand complementary DNA (cDNA) was amplified with specific primers for the coding sequence of *AGO2*. The primers were as follows: forward, 5′-CCAGCATACTACGCTCACCT-3′; reverse, 5′-CAGAGTGTCTTGGTGAACCTG-3′. We quantified *AGO2* mRNA with EXPRESS SYBR Green ER qPCR Supermix Universal (Invitrogen) according to the manufacturer's instructions. Amplification and detection were performed using the Mx3000P Multiplex quantitative PCR system (Stratagene, La Jolla, CA). Results were normalized to the transcript levels of the housekeeping reference gene glyceraldehyde-3-phosphate dehydrogenase (*GAPDH*). Three to seven days after transfection, the culture media were collected to examine HBV production in supernatant. HBs antigen was measured quantitatively using the Abbott chemiluminescence immunoassay kit (Abbott Japan, Tokyo, Japan). HBV DNA levels were determined by Cobas TaqMan HBV standardized real-time PCR assay (Roche Molecular Systems, Pleasanton, CA). Results are expressed in log10 international units/ml. We also evaluated viability of cells using the Cell Counting kit-8 (Dojindo Laboratories, Kumamoto, Japan) at 3, 5 and 7 days after transfection, according to the manufacturer's instructions. All assays were performed in triplicate, and the results are expressed as mean ± SD.

Statistical Analysis

All analyses were performed using the R statistical package (http://www.r-project.org). Continuous variables are reported using the median and range. Moderated t statistics or Mann Whitney U tests were used to detect significant associations, as appropriate, and P-values were adjusted for multiple testing based on the false discovery rate.

Results

MiRNA Microarray Results

We performed miRNA microarray analysis to identify HBV-associated differences in serum miRNA profiles between 10 chronic HBV patients and 10 healthy controls (Fig. S1). 26 miRNAs with an absolute log fold change greater than 1.5 were found to be significantly ($P_{FDR} < 0.05$) up-regulated in serum of HBV patients, and 8 miRNAs were significantly down-regulated (Table 2). MiR-122, miR-22, and miR-99a levels were the most strongly up-regulated in serum of HBV-infected patients, and levels of miR-575, miR-125a-3p, and miR-4294 were the most down-regulated. We also examined miRNAs associated with presence of HBe antigen or HBe antibody, but no miRNAs were significant following correction for multiple testing (data not shown).

Analysis of Serum Sample Mixtures from HBV-infected Patients and Healthy Controls

In addition to individual serum samples, we also examined 4 pooled serum samples as follows: 10 healthy males, 10 healthy females, 10 HBV patients with low ALT levels, and 10 HBV patients with high ALT levels (Fig. S2). In agreement with results from individual analysis, miR-122 and miR-99 levels were significantly higher in serum from HBV serum samples compared to healthy control samples (Table 2). Corresponding results with a log change greater than 1.5 were found for several other miRNAs, including miR-22, miR-642b, miR-125b (up-regulated) and miR-575 and miR-4294 (down-regulated), but results were not significant following correction for multiple testing in the mixture samples due to the small number of samples compared.

RT-PCR Analysis

Serum levels of 19 miRNAs were analyzed using quantitative RT-PCR analysis of 250 chronic HBV patients and 20 healthy controls. Several miRNAs (miR-122, miR-22, miR-99a, miR-720, miR-125b, and miR-1275) were significantly up-regulated in

Table 2. Top 10 up- or down-regulated serum miRNAs associated with chronic HBV infection.

Sample	Direction	miRNA	logFC	AveExpr	t	P	P_{FDR}
Serum	Up	hsa-miR-122	5.97	9.09	12.84	3.27E−12	3.06E−09
		hsa-miR-99a	2.59	6.20	10.73	2.11E−10	2.19E−08
		hsa-miR-22	2.49	9.55	10.47	2.10E−10	2.19E−08
		hsa-miR-191	2.19	8.42	11.87	1.68E−11	3.93E−09
		hsa-miR-642b	2.03	10.07	9.93	5.92E−10	4.26E−08
		hsa-miR-125b	1.95	5.99	8.72	9.91E−09	4.21E−07
		hsa-miR-486-3p	1.79	9.09	8.01	3.19E−08	9.95E−07
		hsa-miR-378	1.78	5.97	9.94	9.00E−10	6.02E−08
		hsa-miR-320d	1.70	7.19	7.88	4.25E−08	1.21E−06
		hsa-miR-23b	1.69	8.99	7.62	7.64E−08	1.93E−06
	Down	hsa-miR-575	−2.10	8.35	−10.00	5.20E−10	4.05E−08
		hsa-miR-125a-3p	−1.99	7.22	−11.91	1.56E−11	3.93E−09
		hsa-miR-4294	−1.75	11.82	−11.37	4.07E−11	7.63E−09
		hsa-miR-92a-2*	−1.64	11.03	−7.70	6.36E−08	1.75E−06
		hsa-miR-1202	−1.59	8.60	−12.41	6.72E−12	3.14E−09
		hsa-miR-30c-1*	−1.31	6.29	−8.66	1.12E−08	4.35E−07
		hsa-miR-1275	−1.19	9.91	−7.50	1.00E−07	2.35E−06
		hsa-miR-3197	−1.05	11.46	−8.58	9.24E−09	4.21E−07
		hsa-miR-1908	−1.03	13.75	−9.05	3.49E−09	2.04E−07
Mixture	Up	hsa-miR-122	6.80	9.09	20.51	1.09E−06	0.001
		hsa-miR-99a	2.58	6.34	9.32	9.80E−05	0.037
		hsa-miR-22	2.07	8.60	3.16	0.020	0.528
		hsa-miR-125b	2.03	6.29	5.09	0.002	0.264
		hsa-miR-1915*	1.80	8.32	6.24	0.001	0.158
		hsa-miR-3648	1.69	14.16	5.06	0.002	0.264
		hsa-miR-642b	1.64	9.82	4.49	0.004	0.377
		hsa-miR-1288	1.39	6.43	3.56	0.012	0.528
		hsa-miR-325	1.30	4.91	2.87	0.047	0.586
		hsa-miR-486-3p	1.29	8.98	3.87	0.009	0.480
	Down	hsa-miR-575	−1.95	8.43	−6.38	0.001	0.158
		hsa-miR-4294	−1.79	11.95	−5.99	0.001	0.158
		hsa-miR-654-3p	−1.35	5.36	−2.99	0.042	0.569
		hsa-miR-1202	−1.24	8.52	−3.97	0.008	0.480
		hsa-miR-1237	−1.06	7.52	−3.10	0.022	0.531
		hsa-miR-744	−1.03	9.51	−2.91	0.028	0.545

Expression levels were compared using moderated t-statistics, and P-values were corrected for multiple testing using the false discovery rate.
logFC: log2 fold-change between patients with chronic HBV infection relative to healthy individuals.
AveExpr: The average log2 expression level for each miRNA over all samples.
t: moderated t-statistic for patients with chronic HBV infection compared to healthy individuals P for each miRNA.
P: uncorrected P-value for t-test.
P_{FDR}: P-value adjusted for multiple testing based on the false discovery rate.
doi:10.1371/journal.pone.0047490.t002

serum from HBV-infected patients (Table 3). Agreement of microarray and RT-PCR results was strongest for up-regulation of miR-122, miR-22, and miR-125b in serum of HBV patients. To determine whether there is a linear relationship between HBV markers and HBV-associated miRNAs, we analyzed the correlation between HBsAg and 6 up-regulated miRNAs. MiR-122, miR-99a, and miR-125b levels were found to be significantly correlated with HBsAg levels with $R^2>0.5$ (Fig. S3). These three miRNAs were also significantly correlated with HBV DNA titers, with R^2 of about 0.4 (Fig. S4). MiR-122 and miR-22 were significantly but diffusely associated with serum ALT levels ($R^2>0.2$; Fig. S5). To identify miRNAs associated with different phases of HBV infection, we also analyzed the 6 significantly up-regulated miRNAs with respect to the presence of HBe antigen and antibody. MiR-122, miR-99a, miR-720, and miR-125b were each highly significantly elevated in chronic HBV patients who were positive for the HBe antigen ($P<4.0E-07$; Fig. S6). Similarly, each miRNA was significantly elevated in chronic HBV patients who were negative for the HBe antibody ($P<9.1E-05$; Fig. S7).

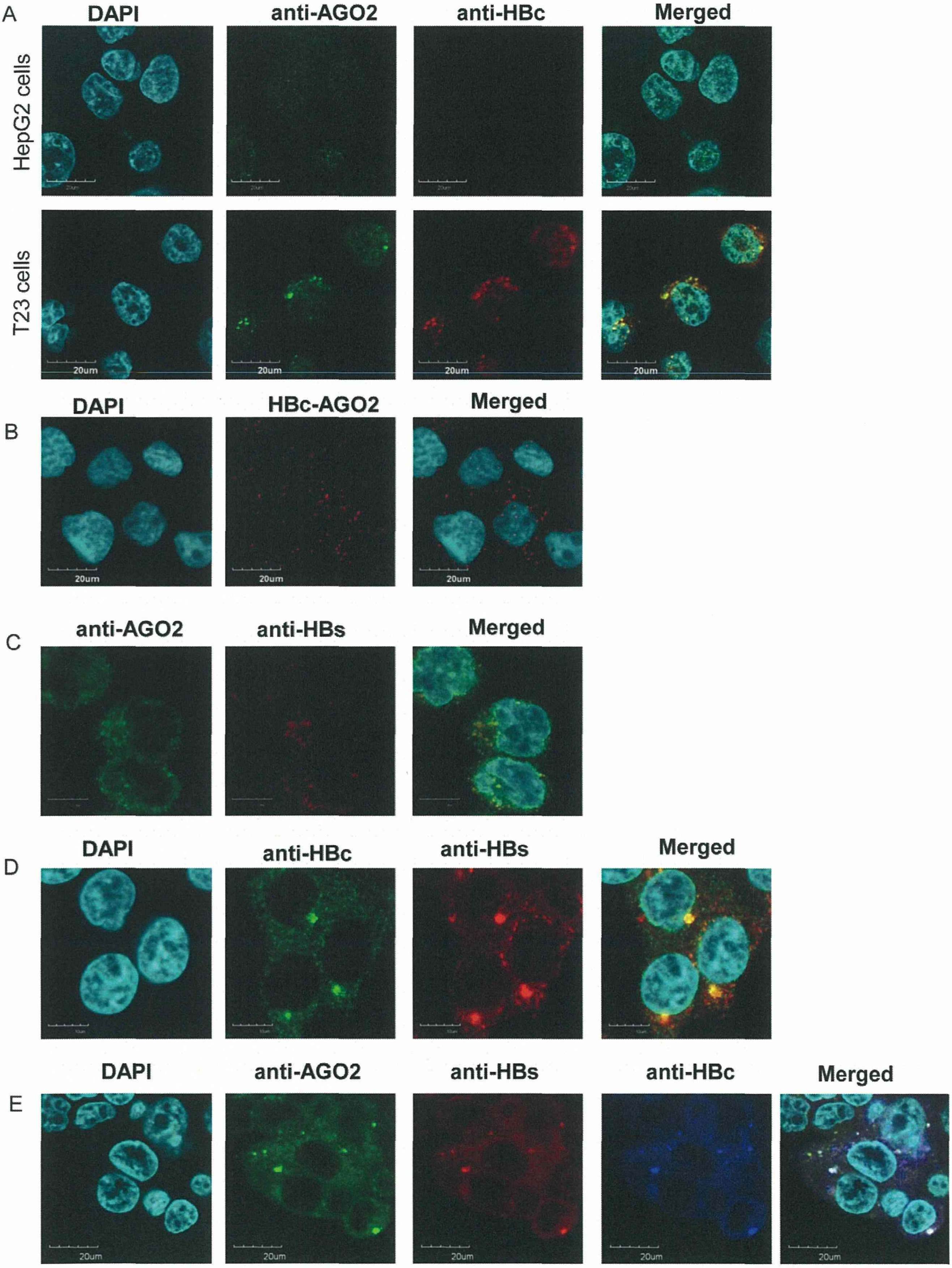
A
DAPI
anti-AGO2
anti-HBc
Merged
HepG2 cells
T23 cells
20um
B
DAPI
HBc-AGO2
Merged
20um
C
anti-AGO2
anti-HBs
Merged
D
DAPI
anti-HBc
anti-HBs
Merged
E
DAPI
anti-AGO2
anti-HBs
anti-HBc
Merged
20um

Figure 1. Co-localization of HBcAg and HBsAg with AGO2 in stably transfected T23 cells. A) Anti-AGO2 and anti-HBc staining overlapped in stably transfected T23 cells, but not in HepG2 control cells, suggesting an interaction between HBc and AGO2. B) HBc-AGO2 was detected in T23 but not HepG2 cells using proximity ligation assays (PLA), suggesting a protein-protein interaction between HBcAg and AGO2. C) Overlap of anti-AGO2 and anti-HBs staining suggests co-localization of HBs and AGO2. D) Anti- HBc, and anti-HBs staining overlapped in T23 cells, which may indicate that HBc and HBs co-localize. E) Overlap of anti-AGO2, anti-HBc, and anti-HBs staining in T23 cells suggests that all three proteins may co-localize.
doi:10.1371/journal.pone.0047490.g001

Pathway Analysis

Predicted gene targets of up-regulated miRNAs were most strongly associated with the GO term PROTEIN_TYROSINE_PHOSPHATASE_ACTIVITY (P = 5.24E−3), and down-regulated miRNAs were associated with the term POSITIVE_REGULATION_OF_JNK_ACTIVITY (P 9.47e−4). Predicted target genes associated with phosphatase activity and dephosphorylation included MTMR3, PTPN18, DUSP5, PTPN2, DUSP2, and PPP1CA.

MiRNA Expression in Liver Biopsy Samples

We compared miRNA expression in non-cancerous liver biopsy samples from a patient with chronic HBV to two uninfected patients (Table S2, Fig. S8). MiRNA levels were highly correlated between liver tissue and serum in all patients (P = <0.001; $R^2 = 0.57$), including the top HBV-associated miRNAs identified by microarray and RT-PCR analysis in this study.

Co-localization of HBcAg and HBsAg with AGO2

Using immunocytochemistry and PLA analysis, we found that HBV core protein and AGO2 co-localized within T23 cells (Fig. 1A–B), suggesting a potential protein-protein interaction between HBcAg and AGO2. AGO2 also co-localized with HBs in T23 cells (Fig. 1C), indicating a potential interaction between HBs and AGO2. Overlap between anti-HBc and anti-HBs staining (Fig. 1D) and between anti-AGO2, anti-HBc, and anti-HBs (Fig. 1E) suggests that these three proteins may co-localize. No overlap was observed between anti-AGO2 and anti-HBx staining in HepG2 cells transfected with HBx expression plasmid (p3FLAG-HBx) nor in control cells, suggesting that HBx does not interact with AGO2 (data not shown).

Subcellular Localization

We also examined HBcAg sub-cellular localization using immunocytochemistry and PLA analysis and found that HBcAg localized to several intracellular compartments, including the ER, autophagosomes, endosomes, and Golgi (Fig. 2). No evidence was found for interaction with mitochondria (data not shown). Using immunocytochemistry, HBsAg was also found to localize diffusely to several intracellular compartments, including the ER, endosomes, autophagosomes, Golgi, mitochondria, processing bodies, multi-vesicular bodies, and the nuclear envelope (Fig. 3). HBx localized non-specifically in the nucleus and cytoplasm, and no sub-cellular location could be ascertained (Fig. S9).

RNA Interference against AGO2

Antisense RNA directed against AGO2 strongly suppressed AGO2 expression (Fig. 4A) and resulted in lower HBV DNA (Fig. 4B) and HBsAg (Fig. 4C) levels in the supernatant. Cell viability was not significantly reduced (Fig. 4D).

Discussion

In this study, we report a set of miRNAs that were up-regulated in serum of HBV infected individuals compared to healthy

Table 3. Quantitative RT-PCR results of selected miRNAs associated in serum of chronic HBV patients.

Factor	Total (n = 270)	HBV (n = 248)	Healthy (n = 22)	P
hsa-miR-122/cel-miR-238	0.1513 (0.0068–2.5)	0.1635 (0.0068–2.5)	0.02074 (0.013–0.04)	1.19E−13
hsa-miR-22/cel-miR-238	0.3 (0.06–1.7)	0.3028 (0.06–1.7)	0.2252 (0.11–0.48)	6.35E−03
hsa-miR-99a/cel-miR-238	0.09121 (0.0046–2.4)	0.102 (0.0086–2.4)	0.0136 (0.0046–0.051)	4.61E−12
hsa-miR-720/cel-miR-238	0.1206 (0.024–3.7)	0.1345 (0.031–3.7)	0.04274 (0.024–0.12)	8.93E−11
hsa-miR-125b/cel-miR-238	0.09732 (0.0066–3.1)	0.1131 (0.0066–3.1)	0.02255 (0.0066–0.05)	1.92E−11
hsa-miR-1275/cel-miR-238	0.4842 (0.099–1.6)	0.5046 (0.099–1.6)	0.4044 (0.24–0.6)	0.010781066
hsa-miR-1826/cel-miR-238	0.5023 (0.14–4.6)	0.5583 (0.26–4.6)	0.33 (0.14–1.4)	7.23E−03
hsa-miR-1308/cel-miR-238	2.831 (1.1–6.9)	2.578 (1.1–6.9)	3.113 (2.3–4.7)	0.223164946
hsa-miR-923/cel-miR-238	3.8 (1.8–9.6)	4.141 (1.8–9.6)	3.01 (2–5)	0.104331611
hsa-miR-1280/cel-miR-238	1.089 (0.36–5)	1.332 (0.6–5)	0.5275 (0.36–0.8)	1.06E−05
hsa-miR-26a/cel-miR-238	1.221 (0.34–3.4)	1.221 (0.34–3.4)	1.231 (0.82–2.4)	0.532171224
hsa-let-7a/cel-miR-238	0.9608 (0.2–2.5)	0.9211 (0.2–2.5)	1.074 (0.71–1.9)	0.235258945
hsa-let-7f/cel-miR-238	1.134 (0.052–2.6)	1.126 (0.052–2.6)	1.143 (0.8–1.7)	0.639411853
hsa-let-7d/cel-miR-238	1.147 (0.35–1.9)	1.106 (0.35–1.8)	1.231 (0.73–1.9)	2.88E−01
hsa-miR-638/cel-miR-238	1.23 (0.3–7)	1.082 (0.3–7)	1.366 (0.68–4)	0.288244047
hsa-miR-1908/cel-miR-238	1.369 (0.45–3.2)	1.357 (0.45–1.9)	1.447 (0.7–3.2)	0.370765019
hsa-miR-34a/cel-miR-238	0.07502 (0.013–1.2)	0.108 (0.026–1.2)	0.02738 (0.013–0.044)	1.41E−05
hsa-miR-886-5p/cel-miR-238	1.627 (0.54–3.6)	1.773 (0.54–3.6)	1.55 (0.97–2.7)	0.478520977

Expression levels were compared using the Mann-Whitney U test.
doi:10.1371/journal.pone.0047490.t003